Diruthenium−Tin Complexes from the Reaction of Ph_2SnH_2 with $Ru(CO)_5$ and Their Reactions with Bis(tri-*tert*-butylphosphine)platinum

Richard D. Adams* and Eszter Trufan

Department of Chemistry and Biochemistry, University of South Carolina, Columbia, South Carolina 29208

Received May 1, 2008

Ph_2SnH_2 reacts with 2 equiv of $Ru(CO)_5$ to give the compound $[Ru(CO)_4H]_2(\mu\text{-}SnPh_2)$ (**1**) in 57% yield by loss of CO from each molecule of $Ru(CO)_5$ and by an oxidative addition of an Sn−H bond to each ruthenium atom. When compound **1** was irradiated with visible radiation, the compound $Ru_2(CO)_8(\mu\text{-}SnPh_2)$ (**2**) was obtained by loss of hydrogen. A mechanism involving loss of CO followed by loss of H_2 and readdition of CO is supported by isotopic labeling studies. Compound **1** reacts with $Pt(PBu^t_3)_2$ to yield the new trimetallic compound $Ru_2(CO)_7(\mu\text{-}SnPh_2)(\mu\text{-}H)_2(\mu\text{-}PtPBu^t_3)$ (**3**). Compound **3** contains a $Pt(CO)(PBu^t_3)$ group bridging the Ru−Ru bond and two bridging hydrido ligands. Compound **2** reacts with $Pt(PBu^t_3)_2$ to yield the two products $PtRu_2(CO)_8)(PBu^t_3)(\mu\text{-}SnPh_2)$ (**4**; 78% yield) and $Pt_2Ru_2(CO)_8(PBu^t_3)_2(\mu\text{-}SnPh_2)$ (**5**; 15% yield) by the addition of one and two $Pt(PBu^t_3)$ groups to the metal−metal bonds of **2**. The first $Pt(PBu^t_3)$ addition occurs at the Ru−Ru bond to form **4**. The second $Pt(PBu^t_3)$ addition occurs at one of the Ru−Sn bonds. Compound **4** reacts with hydrogen under irradiation with visible light to yield **3**. Fenske−Hall molecular orbitals were calculated for the compounds **2**−**5**. The molecular orbital analysis of **2** explains the nature of the addition of the $Pt(PBu^t_3)$ groups to its metal−metal bonds. The molecular structures of **1**−**5** were determined by single-crystal X-ray diffraction analysis.

Introduction

In recent studies we have shown that the tin hydride compound Ph_3SnH reacts readily with polynuclear metal carbonyl cluster complexes to yield higher nuclearity cluster complexes containing large numbers of tin-containing ligands (eqs 1–3).[1–3] The bridging tin ligands $SnPh_2$,[1–5] SnPh,[2,3] and even naked Sn[6] are commonly formed by the cleavage of one to three of the Ph groups from the tin atom.

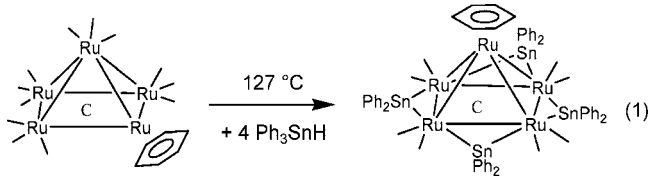

(1)

It has been shown that some of these tin-containing complexes can serve as precursors to di- and trimetallic nanoparticles that exhibit high activity and selectivity for certain types of catalytic hydrogenation reactions.[2,7]

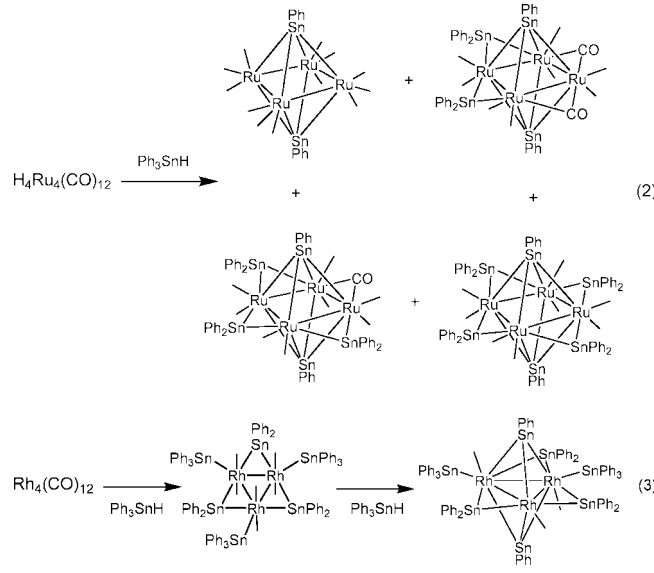

We have also found that it is possible to add $Pd(PBu_3^t)$ and $Pt(PBu_3^t)$ groups to transition-metal−tin bonds by reactions with the compounds $Pd(PBu_3^t)_2$ and $Pt(PBu_3^t)_2$: e.g., eqs 4[8] and 5.[4]

We have also found that $Pd(PBu^t_3)_2$ and $Pt(PBu^t_3)_2$ can activate the M−H bond of the tin-containing metal carbonyl

* To whom correspondence should be addressed. E-mail: Adams@mail.chem.sc.edu.

(1) Adams, R. D.; Captain, B.; Fu, W.; Smith, M. D. *Inorg. Chem.* **2002**, *41*, 2302–2303.
(2) Adams, R. D.; Boswell, E. M.; Captain, B.; Hungria, A. B.; Midgley, P. A.; Raja, R.; Thomas, J. M. *Angew. Chem., Int. Ed.* **2007**, *46*, 8182–8185.
(3) Adams, R. D.; Captain, B.; Hall, M. B.; Webster, C. E. *Inorg. Chem.* **2004**, *43*, 7576–7578.
(4) Adams, R. D.; Captain, B.; Herber, R. H.; Johansson, M.; Nowik, I., Jr.; Smith, M. D. *Inorg. Chem.* **2005**, *44*, 6346–6358.
(5) Adams, R. D.; Captain, B.; Zhu, L. *Organometallics* **2006**, *25*, 2049–2054.
(6) Adams, R. D.; Captain, B.; Zhu, L. *Organometallics* **2006**, *25*, 4183–4187.
(7) (a) Hungria, A. B.; Raja, R; Adams, R. D.; Captain, B.; Thomas, J. M.; Midgley, P. A.; Golvenko, V.; Johnson, B. F. G. *Angew. Chem., Int. Ed.* **2006**, *45*, 4782–4785. (b) Thomas, J. M.; Johnson, B. F. G.; Raja, R.; Sankar, G.; Midgley, P. A. *Acc. Chem. Res.* **2003**, *36*, 20–30.
(8) Adams, R. D.; Captain, B.; Hall, M. B.; Trufan, E.; Yang, X. *J. Am. Chem. Soc.* **2007**, *129*, 12328–12340.

10.1021/om800385w CCC: $40.75 © 2008 American Chemical Society
Publication on Web 07/23/2008

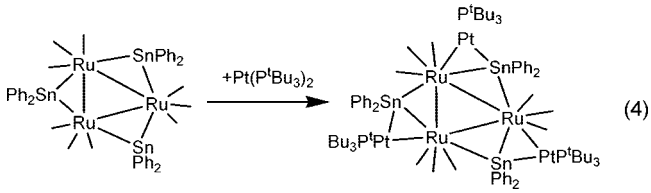

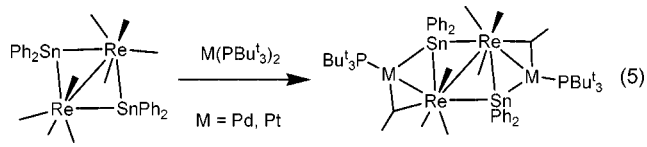

hydride complexes $HM(CO)_4SnPh_3$ (M = Ru, Os) toward insertion of alkynes into the metal−hydrogen bond. It was shown that the $M(PBu^t_3)$ group (M = Pd, Pt) activates the M−H bond by forming a complex to it prior to the addition/insertion of the alkyne: e.g., eq 6.[9]

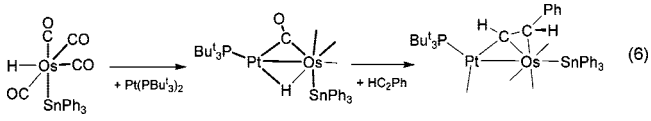

We have now investigated the reaction of Ph_2SnH_2 with $Ru(CO)_5$ and have obtained the new diruthenium−tin complex $[Ru(CO)_4H]_2(\mu\text{-}SnPh_2)$ (**1**) by oxidative addition of the Sn−H bonds to the ruthenium atoms. Compound **1** loses hydrogen upon irradiation to yield the compound $Ru_2(CO)_8(\mu\text{-}SnPh_2)$ (**2**). The synthesis and characterization of these compounds and investigations of their reactions with $Pt(PBu^t_3)_2$ are described in this report.

Experimental Section

General Data. All the reactions were performed under a nitrogen atmosphere by using the standard Schlenk techniques. Reagent grade solvents were dried by the standard procedures and were freshly distilled prior to use. Infrared spectra were recorded on an AVATAR 360 FT-IR spectrophotometer. ^{1}H NMR and ^{31}P NMR were recorded on a Varian Mercury 400 spectrometer operating at 399 and 162 MHz, respectively. ^{31}P NMR spectra were externally referenced against 85% ortho-H_3PO_4. Mass spectrometric measurements were performed on a VG 70S instrument by using direct exposure probe and electron impact ionization (EI). $Ru_3(CO)_{12}$ and $Pt(PBu^t_3)_2$ were purchased from Strem and were used without further purifications. Ph_2SnH_2 was prepared according to a previously published procedure.[10] Product separations were performed in air by TLC on glass plates by using Analtech silica gel 60 Å F254, 0.25 mm thickness.

Synthesis of $[Ru(CO)_4H]_2(\mu\text{-}SnPh_2)$ (1). A solution of $Ru(CO)_5$ was prepared and used in situ as follows:[11] a 51.7 mg amount of $Ru_3(CO)_{12}$ (0.081 mmol) was dissolved in 120 mL of hexane in a 250 mL Pyrex three-neck flask. The solution was placed in an ice bath and irradiated using a medium-pressure mercury UV lamp (1000 W) in the presence of a slow purge of carbon monoxide (CO) for approximately 25 min. During this time the orange solution turned colorless. The reaction flask was then evacuated and refilled with nitrogen to remove the excess CO. A 70.0 mg amount of H_2SnPh_2 (0.254 mmol) was then added to the $Ru(CO)_5$ solution at 0 °C. The solution was then heated to reflux for 30 min, during which time the colorless solution turned orange. After cooling, the solvent was removed in vacuo and the product was purified by TLC by using a 6:1 hexane−methylene chloride solvent mixture to yield 48.8 mg (57%) of pale orange **1**. *Note:* the TLC separation should be performed in the dark, because compound **1** is light sensitive. Spectral data for **1** are as follows. IR ν_{CO} (cm^{-1} in hexane): 2119 (w), 2105 (s), 2057 (s, sh), 2045 (vs), 2038 (s, sh), 2026 (s, sh). ^{1}H NMR ($CDCl_3$, in ppm): δ 7.22−7.65 (m, 10 H, Ph), −7.63 (s, 2H, hydride, $^2J_{119}$Sn−H = 55 Hz, $^2J_{117}$Sn−H = 52.2 Hz). EI-MS: *m/z* 702 M^+ (parent ion, weak); 674, $M^+ - CO$; 644, $M^+ - 2CO - H_2$; 616, $M^+ - 3CO - H_2$; 560, $M^+ - 5CO - H_2$; 532, $M^+ - 6CO - H_2$; 504, $M^+ - 7CO - H_2$; 476, $M^+ - 8CO - H_2$.

Irradiation of 1 under CO. A 15.4 mg amount of **1** was dissolved in 15 mL of benzene in a 100 mL three-neck flask. The pale yellow solution was irradiated with a 100 W sunlamp for 35 min under a CO atmosphere. The reaction was monitored by IR spectroscopy and was stopped when the peaks corresponding to the starting material had disappeared. The solvent was then removed in vacuo, and the product was isolated by TLC by using a 6:1 hexane−methylene chloride solvent mixture to yield 7.9 mg (51%) of pale yellow $Ru_2(CO)_8(\mu\text{-}SnPh_2)$ (**2**). *Note:* the TLC separation should be performed in the dark, because **2** is light sensitive. Spectral data for **2** are as follows. IR ν_{CO} (cm^{-1} in hexane): 2107 (w), 2066 (s), 2045 (vs), 2037 (m, sh), 2028 (vs), 2021 (w, sh), 2011 (w), 1999 (w). ^{1}H NMR ($CDCl_3$, in ppm): δ 7.22−7.65 (m, 10 H, Ph). EI-MS: *m/z* 700 (parent ion).

Irradiation of 1 under N_2 in an NMR Tube. A 38.6 mg amount of **1** was dissolved in d_6-benzene in a NMR tube. The NMR tube was evacuated and then filled with nitrogen. The purity of the starting material was confirmed by ^{1}H NMR. The solution in the tube was then irradiated with a 100 W sunlamp for 50 min. After this time, another ^{1}H NMR spectrum was recorded. This spectrum showed a prominent peak at 4.46 ppm that corresponds to the chemical shift of H_2 in d_6-benzene. The solvent was then removed in vacuo, and the product was separated by TLC by using a 6:1 hexane−methylene chloride solvent mixture to yield 5.2 mg (14%) of pale yellow **2**.

Preparation of $Ru_2(CO)_7(\mu\text{-}SnPh_2)(\mu\text{-}H)_2(\mu\text{-}PtPBu^t_3)$ (3). A 14.0 mg (0.020 mmol) amount of **1** was dissolved in 30 mL of hexane in a 100 mL three-neck flask. To this solution was added a 12.0 mg (0.020 mmol) amount of $Pt(PBu^t_3)_2$, and the mixture was stirred at room temperature for 10 min. The pale yellow solution turned orange. The solvent was then removed in vacuo, and the product was purified by TLC by using a 6:1 hexane−methylene chloride solvent mixture to yield 14.6 mg (76%) of orange $Ru_2(CO)_7(\mu\text{-}SnPh_2)(\mu\text{-}H)_2(\mu\text{-}PtPBu^t_3)$ (**3**). Spectral data for **3** are as follows. IR ν_{CO} (cm^{-1} in hexane): 2070 (m), 2043 (s), 2007 (m), 1987 (m, sh). ^{1}H NMR ($CDCl_3$, in ppm): δ 7.16−7.53 (m, 10H, Ph), 1.17 (d, 27H, CH_3, $^3J_{P-H}$ = 13 Hz), −11.63 (t, 1H, hydride, $^2J_{H-H}$ = 2.3 Hz), −12.44 (dd, 1 H, hydride, $^2J_{H-H}$ = 2.3 Hz, $^3J_{P-H}$ = 13 Hz). EI-MS: *m/z* 1072 (parent ion).

Preparation of $PtRu_2(CO)_8)(PBu^t_3)(\mu\text{-}SnPh_2)$ (4) and $Pt_2Ru_2(CO)_8)(PBu^t_3)_2(\mu\text{-}SnPh_2)$ (5). An 11.0 mg (0.016 mmol) amount of **2** was dissolved in 20 mL of methylene chloride in a 100 mL three-neck flask. To this solution was added 10.0 mg (0.017 mmol) of $Pt(PBu^t_3)_2$, and the mixture was stirred for 70 min at room temperature in the dark. During this time the starting pale yellow solution turned to a dark orange. The solvent was then removed, and the products were separated by TLC by using a 6:1 hexane−methylene chloride solvent mixture to yield 13.5 mg of orange **4** (78%) and 3.5 mg of red **5** (15%) Spectral data for **4** are as follows. IR ν_{CO} (cm^{-1} in CH_2Cl_2): 2086 (vw), 2053 (s), 2015 (vs), 1986 (m), 1826 (m), 1810 (m). ^{1}H NMR ($CDCl_3$, in ppm): δ 7.33−7.66 (m, 10H, Ph), 1.51 (d, 27H, CH_3, $^3J_{P-H}$ = 13 Hz). ^{31}P{^{1}H} NMR (in $CDCl_3$, ppm): δ 107.02 (s, 1P, $^1J_{Pt-P}$ = 4901 Hz). EI-MS: *m/z* 1098 (parent ion). Spectral data for **5** are as

(9) Adams, R. D.; Captain, B.; Trufan, E.; Zhu, L. *J. Am. Chem. Soc.* **2007**, *129*, 7545–7556.

(10) Hernán, A.; Horton, P.; Hursthouse, M. B.; Kilburn, J. D. *J. Organomet. Chem.* **2006**, *691*, 1466–1475.

(11) Huq, R.; Poë, A. J.; Chawla, S. *Inorg. Chim. Acta* **1980**, *38*, 121–125.

follows. IR ν_{CO} (cm^{-1} in CH_2Cl_2): 2073 (vw), 2040 (w), 2004 (vs), 1977 (w, sh), 1841 (m), 1815 (m). ^1H NMR ($CDCl_3$, in ppm): δ 7.30−7.91 (m, 10H, Ph), 1.59 (d, 27H, CH_3, $^3J_{P-H}$ = 13 Hz), 1.49 (d, 27H, CH_3, $^3J_{P-H}$ = 13 Hz). $^{31}P\{^1H\}$ NMR (in CD_2Cl_2, ppm): δ 111.47 (s, 1P, $^1J_{Pt-P}$ = 5876 Hz), 108.26 (s, 1P, $^1J_{Pt-P}$ = 4849 Hz). Positive ion ES-MS: *m*/*z* 1495 (M + H, parent ion).

Reaction of $Ru_2(CO)_8(\mu$-$SnPh_2)$ with 2 Equiv of $Pt(PBu^t_3)_2$. A 9.1 mg (0.013 mmol) amount of $Ru_2(CO)_8(\mu$-$SnPh_2)$ was dissolved in 25 mL of methylene chloride in a 100 mL three-neck flask. To this solution was added 17.6 mg (0.294 mmol) of $Pt(PBu^t_3)_2$, and the mixture was stirred for 20 min at room temperature in the dark. During this time, the pale yellow solution turned red. The solvent was then removed, and the products were separated by TLC by using a 6:1 hexane−methylene chloride solvent mixture to give 13.2 mg of red **5** (68% yield).

Irradiation of 1 under ^{13}CO. A 23.6 mg amount of **1** was dissolved in 25 mL of benzene in a 100 mL three-neck flask. The pale yellow solution was irradiated with a 100 W sunlamp for 35 min while a very slow purge of ^{13}CO was applied. The reaction mixture was cooled, and the solvent was removed in vacuo. The products were separated by TLC by using a 6:1 hexane−methylene chloride solvent mixture in the dark. This procedure gave 4.3 mg of **1** and 1.3 mg of **2**. Both products were then analyzed by mass spectrometry, and both showed an enrichment in ^{13}CO to approximately 25% of the total CO composition.

Irradiation of 2 under ^{13}CO. A 7.1 mg amount of **2** was dissolved in 20 mL of benzene in a 100 mL three-neck flask. The solution was stirred in the dark for 30 min under a ^{13}CO atmosphere, and careful IR monitoring showed no sign of change. Then, the solution was irradiated with a 100 W sunlamp for 35 min. The reaction was stopped, the solvent was removed in vacuo, and the products were separated by TLC by using a 6:1 hexane−methylene chloride solvent mixture in the dark. A 2.9 mg portion of the starting material was recovered and was then analyzed by mass spectrometry; it was found to have an enrichment in ^{13}CO to approximately 10% of the total CO composition.

Reaction of 3 with CO. A 13.3 mg (0.012 mmol) amount of **3** was dissolved in 15 mL of benzene in a 100 mL three-neck flask and stirred and irradiated with a 100 W sunlamp under a CO atmosphere for 35 min. The solvent was then removed in vacuo, and the products were separated by TLC by using a 6:1 hexane−methylene chloride solvent mixture to give 8.9 mg of **4** (65% yield).

Reaction of 4 with H_2. A 6.3 mg amount (0.006 mmol) of **4** was dissolved in 14 mL of benzene in a 100 mL three-neck flask and stirred and irradiated with a 100 W sun lamp under an H_2 atmosphere for 40 min. The irradiation was then stopped and the solvent removed in vacuo. The product **3** was then separated by TLC by using a 6:1 hexane−methylene chloride solvent mixture to give 1.3 mg (21% yield).

Reaction of 4 with $Pt(PBu^t_3)_2$. A 17.8 mg amount (0.0162 mmol) of $Ru_2(CO)_8(\mu$-$SnPh_2)(\mu$-$PtPBu^t_3)$ was dissolved in 25 mL of dichloromethane in a 100 mL three-neck flask and stirred for 60 min at room temperature. The solvent was then removed in vacuo, and the products were separated by TLC by using a 6:1 hexane−methylene chloride solvent mixture to give 0.7 mg of unreacted **4** and 20.7 mg (85% yield) of **5**.

Crystallographic Analyses. Orange single crystals of **1**−**3** suitable for X-ray diffraction were obtained by slow evaporation of solvent from solutions in hexane solvent at −80 °C. Orange single crystals of **4** suitable for X-ray diffraction were obtained by slow evaporation of solvent from solutions in methylene chloride−octane solvent mixtures at −25 °C. Red single crystals of **5** suitable for X-ray diffraction were obtained by slow evaporation of solvent from solutions in methylene chloride−octane solvent mixtures at −25 °C. Each data crystal was glued onto the end of a thin glass fiber. X-ray intensity data were measured by using a Bruker SMART APEX CCD-based diffractometer using Mo Kα radiation (λ = 0.710 73 Å). The raw data frames were integrated with the SAINT+ program by using a narrow-frame integration algorithm.[12] Correction for Lorentz and polarization effects were also applied with SAINT+. An empirical absorption correction based on the multiple measurement of equivalent reflections was applied using the program SADABS. All structures were solved by a combination of direct methods and difference Fourier syntheses and refined by full-matrix least squares on F^2, using the SHELXTL software package.[13] All non-hydrogen atoms were refined with anisotropic thermal parameters. Unless indicated otherwise, the hydrogen atoms were placed in geometrically idealized positions and included as standard riding atoms during the least-squares refinements. Crystal data, data collection parameters, and results of the refinements are given in Table 1.

Compounds **1**, **2**, and **5** crystallized in the triclinic crystal system. The space group $P\bar{1}$ was assumed and confirmed by the successful refinement and solution of the structure in each case. The asymmetric crystal unit of **1** contains two independent formula equivalents of the molecule. The hydrido ligands in **1** were located and refined in the analysis. Compound **5** contains one formula equivalent of the molecule in the asymmetric crystal unit and also one and a half molecule of octane from the crystallization solvent that had cocrystallized with the complex. The octane solvent molecule was included in the analysis and was satisfactorily refined with isotropic thermal parameters. The hydrogen atoms on this octane molecules were omitted in these calculations. Compounds **3** and **4** both crystallized in the monoclinic crystal system. The systematic absences in the intensity data identified the space group uniquely as $P2_1/c$ in both cases. For compound **3** there is one formula equivalent of the complex present in the asymmetric unit. One-fourth of a methylene chloride molecule from the crystallization solvent cocrystallized with the complex. It was satisfactorily refined in the analysis. Compound **4** contains four independent formula equivalents of the molecule in the asymmetric unit. All four molecules were located and refined with anisotropic thermal parameters for the non-hydrogen atoms. The carbon atoms on one of the phenyl groups and a few of the *tert*-butyl carbon atoms exhibited large thermal parameters, which was probably due to minor disorder effects.

Molecular Orbital Calculations. All molecular orbital calculations reported herein were performed by using the Fenske−Hall method.[14] The calculations were performed utilizing a graphical user interface developed[15] to build inputs and view outputs from standalone Fenske−Hall and MOPLOT2 binary executables.[16] Contracted double-ζ basis sets were used for the Ru 4d, Pt 5d, Sn 5p, P 3p, and C and O 2p atomic orbitals. The Fenske−Hall scheme is a nonempirical approximate method that is capable of calculating molecular orbitals for very large transition-metal systems. For these calculations, the input structures were obtained from the positional parameters from the crystal structure analyses. The structures are not optimized by these calculations. The *tert*-butyl groups on the phosphine ligands and the phenyl groups on the $SnPh_2$ ligand were replaced with hydrogen: e.g., PH_3 and SnH_2.

(12) SAINT+ Version 6.2a; Bruker Analytical X-ray Systems, Inc., Madison, WI, 2001.

(13) Sheldrick, G. M. SHELXTL Version 6.1; Bruker Analytical X-ray Systems, Inc., Madison, WI, 1997.

(14) (a) Hall, M. B.; Fenske, R. F. *Inorg. Chem.* **1972**, *11*, 768–775. (b) Webster, C. E.; Hall, M. B. In *Theory and Applications of Computational Chemistry: The First Forty Years*; Dykstra, C., Ed.; Elsevier: Amsterdam, 2005; Chapter 40, pp 1143−1165.

(15) Manson, J.; Webster, C. E.; Hall, M. B. JIMP, development version 0.1.v117 (built for Windows PC and Redhat Linux); Department of Chemistry, Texas A&M University, College Station, TX, 2004; http://www.chem.tamu.edu/jimp/.

(16) Lichtenberger, D. L. MOPLOT2 for orbital and density plots from linear combinations of Slater or Gaussian type orbitals, version 2.0; Department of Chemistry, University of Arizona, Tucson, AZ, 1993.

Table 1. Crystallographic Data for Compounds 1−5

	1	2	3	4	5
empirical formula	$Ru_2SnO_8C_{20}H_{12}$	$Ru_2SnO_8C_{20}H_{10}$	$PtRu_2SnPO_7C_{31}H_{39}\cdot{}^1/_4CH_2Cl_2$	$PtRu_2SnPO_8C_{24}H_{37}$	$Pt_2Ru_2SnP_2O_8C_{44}H_{64}\cdot{}^3/_2C_8H_{18}$
formula wt	701.12	699.11	1091.74	1000.43	1665.24
cryst syst	triclinic	triclinic	monoclinic	monoclinic	triclinic
lattice params					
a (Å)	9.6227(5)	8.2765(4)	16.9915(5)	27.138(2)	13.8149(6)
b (Å)	15.1915(7)	9.3170(5)	11.7343(3)	17.0066(14)	15.2333(7)
c (Å)	17.7393(8)	16.1426(9)	19.2385(6)	32.635(3)	17.0571(8)
α (deg)	75.200(1)	87.377(1)	90.00	90.00	65.136(1)
β (deg)	75.721(1)	75.261(1)	99.409(1)	94.656(2)	84.937(1)
γ (deg)	89.312(1)	75.544(1)	90.00	90.00	70.122(1)
V (Å^3)	2426.1(2)	1147.7(1)	3784.23(19)	15012(2)	3056.5(2)
space group	$P\bar{1}$ (No. 2)	$P\bar{1}$ (No. 2)	$P2_1/c$ (No. 14)	$P2_1/c$ (No. 14)	$P\bar{1}$ (No. 2)
Z	2	2	4	16	2
ρ_{calcd} (g/cm^3)	1.920	2.023	1.916	2.213	1.809
μ(Mo Kα) (mm^{-1})	2.290	2.420	5.238	6.549	5.547
temp (K)	293(2)	293(2)	294(2)	294(2)	150(2)
$2\theta_{max}$ (deg)	56.82	56.52	49.66	57.70	56.64
no. of obsd rflns ($I > 2\sigma(I)$)	9029	4796	6013	20 028	13 486
no. of params	575	280	418	1657	598
goodness of fit GOF[a]	1.039	1.206	1.079	1.009	1.038
max shift in cycle	0.003	0.004	0.001	0.014	0.018
residuals:[a] R1, wR2	0.0424, 0.1104	0.0277, 0.0889	0.0376, 0.0877	0.0531, 0.1113	0.0307, 0.0768
abs cor, max/min	multi-scan, 1.000/0.804	multi-scan, 1.000/0.773	multi-scan, 1.000/0.744	multi-scan, 1.000/0.398	multi-scan, 1.000/0.728
largest peak in final diff map (e/Å^3)	1.385	0.732	1.362	2.600	2.720

[a] $R1 = \sum_{hkl}(||F_o| - |F_c||)/\sum_{hkl}|F_o|$; $wR2 = [\sum_{hkl}w(|F_o| - |F_c|)^2/\sum_{hkl}wF_o^2]^{1/2}$, $w = 1/\sigma^2(F_o)$; $GOF = [\sum_{hkl}w(|F_o| - |F_c|)^2/(n_{data} - n_{vari})]^{1/2}$.

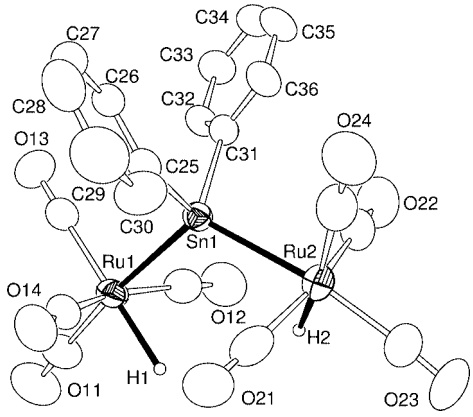

Figure 1. ORTEP diagram of the molecular structure of **1** showing 40% probability thermal ellipsoids. Selected bond distances (Å) and angles (deg) are as follows: molecule 1, Ru(1)−Sn(1) = 2.7206(5), Ru(2)−Sn(1) = 2.7335(6), Ru(1)−H(1) = 1.87(4), Ru(2)−H(2) = 1.57(6); Ru(1)−Sn(1)−Ru(2) = 115.666(18); molecule 2, Ru(3)−Sn(3) = 2.7260(6), Ru(4)−Sn(3) = 2.7219(6), Ru(3)−H(3) = 1.93(4), Ru(4)−H(4) = 1.35(6); Ru(3)−Sn(2)−Ru(4) = 115.866(19).

Results

The compound $[Ru(CO)_4H]_2(\mu\text{-}SnPh_2)$ (**1**) was obtained in 57% yield from the reaction of Ph_2SnH_2 with $Ru(CO)_5$ in hexane solvent when heated to reflux for 30 min. Compound **1** was characterized by IR, ^{1}H NMR, and mass spectra and by a single-crystal X-ray diffraction analysis. There are two crystallographically independent molecules in the asymmetric crystal unit of **1**. Both molecules are structurally similar. An ORTEP diagram of the molecular structure of one of the two independent molecules is shown in Figure 1. The molecule consists of two $HRu(CO)_4$ groups that are held together by a bridging $SnPh_2$ ligand. There is no bond between the ruthenium atoms: Ru(1)···Ru(2) = 4.167(1) Å for molecule 1 and Ru(3)···Ru(4) = 4.167(1) Å for molecule 2. The Ru−Sn bond distances are typical of Ru−Sn single bonds: Ru(1)−Sn(1) = 2.7206(5) Å and Ru(2)−Sn(1) = 2.7335(6) Å for molecule 1 and Ru(3)−Sn(3) = 2.7260(6) Å and Ru(4)−Sn(3) = 2.7219(6) Å for molecule 2. The four CO ligands and the tin atom are arranged in the form of a square pyramid. The sixth ligand on each ruthenium atom is a hydrido ligand that lies trans to the CO ligand in the apex of the square pyramid. The hydrido ligands were located and refined in the structural analysis: Ru(1)−H(1) = 1.87(4) Å, Ru(2)−H(2) = 1.57(6) Å, Ru(3)−H(3) = 1.93(4) Å, and Ru(4)−H(4) = 1.35(6) Å; however, the Ru−H distances span a considerable range, because the hydrido ligands were not located with high precision. The estimated standard deviations are large, because it is difficult to locate hydrogen atoms accurately in the proximity of heavy atoms such as ruthenium. The hydrido ligands exhibit a single high-field resonance at δ −7.63 in the ^{1}H NMR spectrum. The Ru−H and Ru−Sn bond distances are very similar to those observed for the compound $Ru(CO)_4(SnPh_3)H$ (**6**), Ru−H = 1.63(4) Å and Ru−Sn = 2.7108(3) Å, which we recently obtained from the reaction of Ph_3SnH with $Ru(CO)_5$.[9]

When compound **1** was irradiated with visible radiation for 35 min under a CO atmosphere, the new compound $Ru_2(CO)_8(\mu\text{-}SnPh_2)$ (**2**) was formed and isolated in 51% yield. Compound **2** was characterized by IR, ^{1}H NMR, and mass spectra and by a single -crystal X-ray diffraction analysis. An ORTEP diagram of the molecular structure of **2** is shown in Figure 2. The molecule contains two $Ru(CO)_4$ groups that are joined by a Ru−Ru single bond, Ru(1)−Ru(2) = 3.0035(6) Å, and a bridging $SnPh_2$ ligand. The Ru−Ru bond distance is slightly longer than the Ru−Ru bond distance in $Ru_3(CO)_{12}$, 2.854(1) Å.[17] The Ru−Sn bond distances are slightly shorter than those in **1**, Ru(1)−Sn(1) = 2.6596(5) Å, Ru(2)−Sn(1) = 2.6655(5) Å, Ru(1)−Sn(1)−Ru(2) = 68.671(15)°. Although the ruthenium atoms in compounds **1** and **2** obey the 18-electron rule, a Fenske−Hall (FH) molecular orbital analysis of **2** was performed in order to develop a more detailed view of its metal−metal bonding in order to compare with the bonding of

(17) Churchill, M. R.; Hollander, F. J.; Hutchinson, J. P. *Inorg. Chem.* **1977**, *16*, 2655.

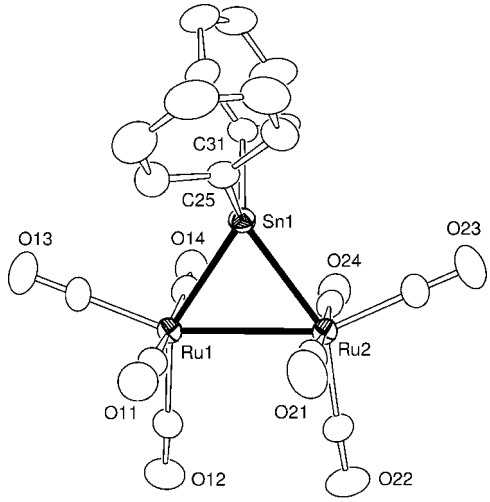

Figure 2. ORTEP diagram of the molecular structure of **2**,showing 30% probability thermal ellipsoids. The hydrogen atoms are omitted for clarity. Selected interatomic bond distances (Å) and angles (deg) are as follows: Ru(1)−Ru(2) = 3.0035(6), Ru(1)−Sn(1) = 2.6596(5), Ru(2)−Sn(1) = 2.6655(5); Ru(1)−Sn(1)−Ru(2) = 68.671(15).

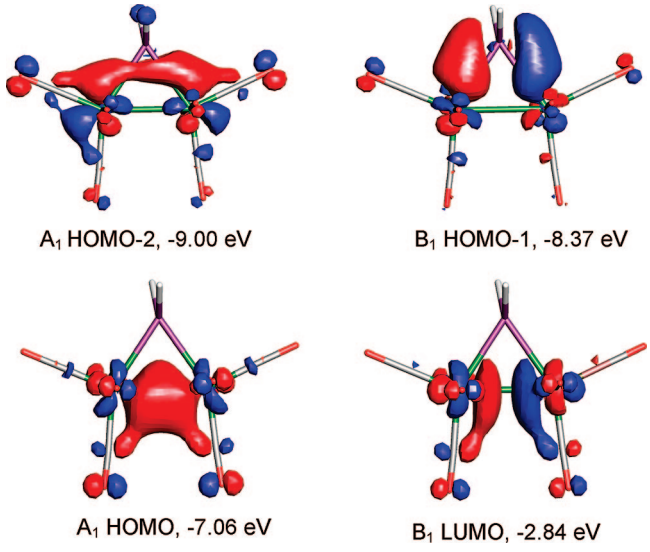

Figure 3. Contour diagrams for the metal−metal bonding molecular orbitals in **2**: A_1 HOMO, B_1 HOMO-1, A_1 HOMO-2, and B_1 LUMO.

its platinum adducts that are described below. The molecular symmetry of **2** is C_{2v}. Contour diagrams of the three highest occupied molecular orbitals (HOMOs) of **2** are shown in Figure 3. The A_1 HOMO lies at −7.07 eV, which is predominantly the Ru−Ru bonding orbital. The Ru−Sn bonds are represented by the B_1 HOMO-1 at −8.37 eV and the A_1 HOMO-2 at −9.00 eV. Their lower energies suggest that the Ru−Sn bonds are stronger than the Ru−Ru bond. The antisymmetric B_1 LUMO in **2** is clearly Ru−Ru antibonding. The importance of M−Sn bonding to bridging $SnPh_2$ ligands was also observed for the related compounds $Rh_3(CO)_6(SnPh_3)_3(\mu\text{-}SnPh_2)_3$[3] and $Re_2(CO)_8(\mu\text{-}SnPh_2)_2$.[18]

In previous work it was shown that the compounds $M(CO)_4(SnPh_3)H$ (M = Ru, Os) are activated by $Pt(PBu^t_3)_2$ and

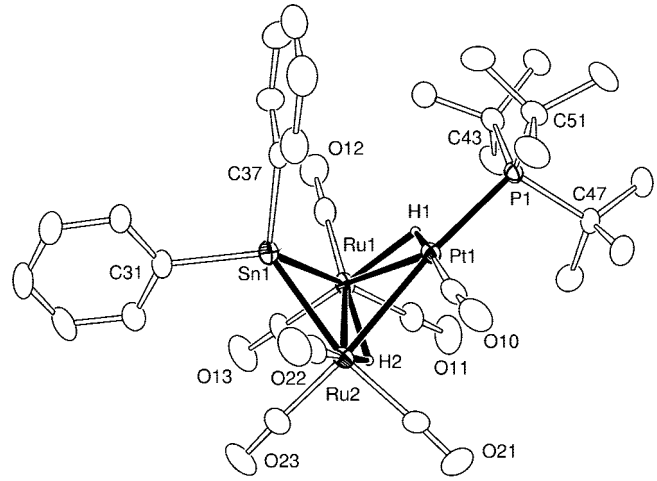

Figure 4. ORTEP diagram of the molecular structure of **3** showing 30% probability thermal ellipsoids. Selected interatomic bond distances (Å) and angles (deg) are as follows: Ru(1)−Ru(2) = 2.9782(8), Pt(1)−Ru(2) = 2.7504(6), Pt(1)−Ru(1) = 2.9404(6), Ru(1)−Sn(1) = 2.6557(8), Ru(2)−Sn(1) = 2.6488(8), Ru(1)−H(1) = 2.09(5), Ru(1)−H(2) = 1.97(7), Ru(2)−H(2) = 1.60(7), Pt(1)−H(1) = 1.37(5), Pt(1)−P(1) = 2.3788(17); Ru(1)−Sn(1)−Ru(2) = 68.31(2), Ru(1)−Pt(1)−Ru(2) = 63.009(18), Sn(1)−Ru(1)−Pt(1) = 71.769(18), Sn(1)−Ru(2)−Pt(1) = 75.012(19).

$Pd(PBu^t_3)_2$ toward the insertion of PhC_2H into their M−H bonds. The nature of the activation was shown by the compound $PtOs(CO)_4(SnPh_3)(PBu^t_3)(\mu\text{-}H)$, which was isolated from the reaction of $Os(CO)_4(SnPh_3)H$ with $Pt(PBu^t_3)_2$ and structurally characterized. The compound $PtOs(CO)_4(SnPh_3)(PBu^t_3)(\mu\text{-}H)$ was found to possess a hydrido ligand bridging a Pt−Os bond. Accordingly, it was decided to investigate the reaction of **1** with $Pt(PBu^t_3)_2$. Compound **1** reacted with $Pt(PBu^t_3)_2$ at room temperature to give the orange product $Ru_2(CO)_7(\mu\text{-}SnPh_2)(\mu\text{-}H)_2(\mu\text{-}PtPBu^t_3)$ (**3**) in 76% yield in 10 min. Compound **3** was characterized by IR, ^1H and ^{31}P NMR, and mass spectra and by a single-crystal X-ray diffraction analysis. An ORTEP diagram of the molecular structure of **3** is shown in Figure 4. The molecule contains two $Ru(CO)_3$ groups that are joined by a hydride-bridged Ru−Ru single bond: Ru(1)−Ru(2) = 2.9782(8) Å. The Ru−Ru bond is also bridged by a $Pt(CO)(PBu^t_3)$ group. The Pt−Ru bond distances are significantly different in length: Pt(1)−Ru(2) = 2.7504(6) Å and Pt(1)−Ru(1) = 2.9404(6) Å. The longer length of the Pt(1)−Ru(1) bond can be attributed to the presence of the bridging hydrido ligand H(1).[19] There is also a $SnPh_2$ ligand bridging the Ru−Ru bond. The Ru−Sn bond distances are very similar to those in **2**: Ru(1)−Sn(1) = 2.6557(8) Å and Ru(2)−Sn(1) = 2.6488(8) Å. There is a second hydrido ligand, H(2), which bridges the Ru−Ru bond. The two hydrido ligands are inequivalent and exhibit separate high-field resonances in the ^1H NMR spectrum,: δ −11.63 (H2) and −12.44 (H1). The latter exhibits significant coupling to the closely positioned phosphorus atom, $^3J_{P-H}$ = 13 Hz.

To develop an understanding of the metal−metal bonding in **3**, a Fenske−Hall (FH) molecular orbital analysis was performed. The contour diagrams of the most important cluster bonding molecular orbitals (HOMOs) are shown in Figure 5. The delocalized bonding of the platinum atom to the two ruthenium atoms is nicely illustrated by the HOMO, which lies at −6.56 eV. The bonding of the tin atom to the two ruthenium

(18) (a) Adamas, R. D.; Captain, B.; Herber, R. H.; Johansson, M.; Nowik, I.; Smith, J. L., Jr.; Smith, M. D. *Inorg. Chem.* **2005**, *44*, 6346–6358. (b) Adams, R. D.; Captain, B.; Johansson, M.; Smith, J. L. *J. Am. Chem. Soc.* **2005**, *127*, 488–489.

(19) (a) Bau, R.; Drabnis, M. H. *Inorg. Chim. Acta* **1997**, *259*, 27–50. (b) Teller, R. G.; Bau, R. *Struct. Bonding* **1981**, *41*, 1–82.

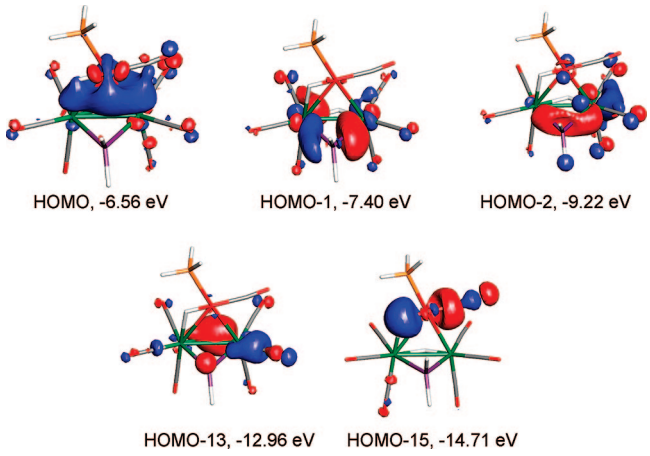

Figure 5. Contour diagrams for the molecular orbitals representing the metal−metal bonding in **3**, HOMO, HOMO-1, and A_1 HOMO-2, and those of the bridging hydrido ligands, HOMO-13 and HOMO-15.

atoms is shown by the symmetric HOMO-2 at −9.22 eV and the antisymmetric HOMO-1 at −7.40 eV. The orbitals involving the bridging hydrido ligands lie at much lower energies. The bonding of the H(1) bridging ligand is shown by the HOMO-15 at −14.71 eV, and the bonding of H(2) to the two ruthenium atoms is shown by the HOMO-13 at −12.96 eV.

It has been shown that the $Pt(PBu^t_3)$ group can be added both to Ru−Sn bonds[7] and to Ru−Ru bonds.[20] Since compound **2** contains both types of these bonds, it was decided to investigate its reaction of $Pt(PBu^t_3)_2$ to try to ascertain if it would be possible to identify any preference for the attachment of the $Pt(PBu^t_3)$ group to these two types of bonds. Two products, $PtRu_2(CO)_8(PBu^t_3)(\mu\text{-}SnPh_2)$ (**4**; 78% yield) and $Pt_2Ru_2(CO)_8(PBu^t_3)_2(\mu\text{-}SnPh_2)$ (**5**; 15% yield), were obtained from the reaction of **2** with $Pt(PBu^t_3)_2$ at room temperature after 70 min. The yield of **5** was increased to 68% when 2 equiv of $Pt(PBu^t_3)_2$ was used in the reaction, and when **4** was treated with an additional quantity of $Pt(PBu^t_3)_2$, it was converted to **5** in 85% yield. Compounds **4** and **5** were both characterized by IR, ^1H and ^{31}P NMR, and mass spectra and by single-crystal X-ray diffraction analyses.

There are four independent molecules in the asymmetric crystal unit of **4**. All four molecules are structurally similar. An ORTEP diagram of one of these four molecules is shown in Figure 6. The molecule is very similar to **2**, except that it contains a $Pt(PBu^t_3)$ group that has been added across the Ru−Ru bond. The Ru−Ru bond distances in **4**, Ru(1)−Ru(2) = 3.0179(10), 3.0168(9), 3.0130(9), 3.0143(10) Å (average 3.0155 Å), are slightly longer than the Ru−Ru distance in **2**, 3.0035(6) Å. The Ru−Sn bond distances in **4** are not significantly different from those in **2**: Ru(1)−Sn(1) = 2.6564(9), 2.6585(9), 2.6586(9), 2.6564(9) Å and Ru(2)−Sn(1) = 2.6533(9), 2.6637(10), 2.6596(9), 2.6588(10) Å. There is a bridging carbonyl ligand across each Ru−Pt bond. The Ru−Pt bond distances, Ru(1)−Pt(1) = 2.7672(8), 2.7750(7), 2.7426(7), 2.7813(8) Å; and Ru(2)−Pt(1) = 2.7681(8), 2.7535(8), 2.7838(7), 2.7683(8) Å (average 2.7675 Å), are slightly shorter than those found for the compound $Ru_3(CO)_{12}[Pt(PBu^t_3)]_3$ (**6**), Ru−Pt (av) = 2.807(1) Å,[20] which has a bridging $Pt(PBu^t_3)$ on each Ru−Ru bond, but in compound **6** only three of the six Ru−Pt distances contain a bridging CO ligand.

(20) Adams, R. D.; Boswell, E. M.; Captain, B.; Zhu, L. *J. Cluster Sci.* **2008**, *19*, 121–132.

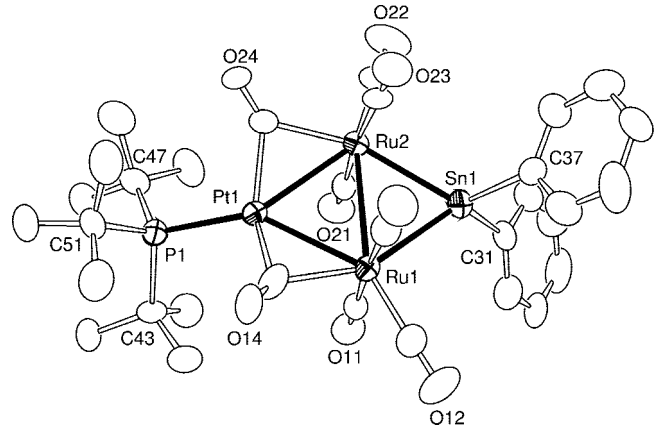

Figure 6. ORTEP diagram of the molecular structure of **4** showing 30% probability thermal ellipsoids. The hydrogen atoms are omitted for clarity. Selected interatomic bond distances (in Å) each of the four independent molecules in the unit cell are as follows: Ru(1)−Ru(2) = 3.0179(10), 3.0168(9), 3.0130(9), 3.0143(10); Ru(1)−Sn(1) = 2.6564(9), 2.6585(9), 2.6586(9), 2.6564(9); Ru(2)−Sn(1) = 2.6533(9), 2.6637(10), 2.6596(9), 2.6588(10); Ru(1)−Pt(1) = 2.7672(8), 2.7750(7), 2.7426(7), 2.7813(8); Ru(2)−Pt(1) = 2.7681(8), 2.7535(8), 2.7838(7), 2.7683(8); Pt(1)−P(1) = 2.353(2), 2.350(2), 2.347(2), 2.367(2).

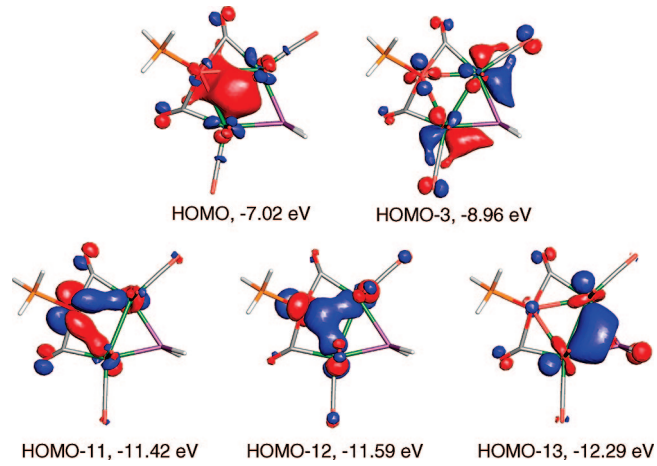

Figure 7. Contour diagrams of the FH molecular orbitals in **4** that show the metal−metal bonding.

To understand the metal−metal bonding in **4**, a Fenske−Hall molecular orbital analysis was performed. Contour diagrams of five selected molecular orbitals in **4** are shown in Figure 7. The HOMO at −7.02 eV exhibits delocalized bonding between the platinum atom and the two ruthenium atoms. This orbital clearly shows how the $Pt(PBu^t_3)$ group interacts with the HOMO of **2**. This explains the preference of the $Pt(PBu^t_3)$ group for addition to the Ru−Ru bond. The bonding between the ruthenium atoms and the bridging tin atom is shown by the antisymmetric HOMO-3 at −8.96 eV and the symmetric HOMO-13 at −12.29 eV. Significant interactions between the platinum atom and the two ruthenium atoms are shown by the symmetric HOMO-12 at −11.59 eV and the antisymmetric HOMO-11 at −11.42 eV. In the presence of mild irradiation, compound **4** reacts with hydrogen by loss of CO to form **3**, but the yield is not high, 21%.

An ORTEP diagram of the molecular structure of **5** is shown in Figure 8. The molecule is very similar to **4** except that it contains a second $Pt(PBu^t_3)$ group that was added across one of the Ru−Sn bonds of **4**. In contrast to **4**, the Ru−Ru bond

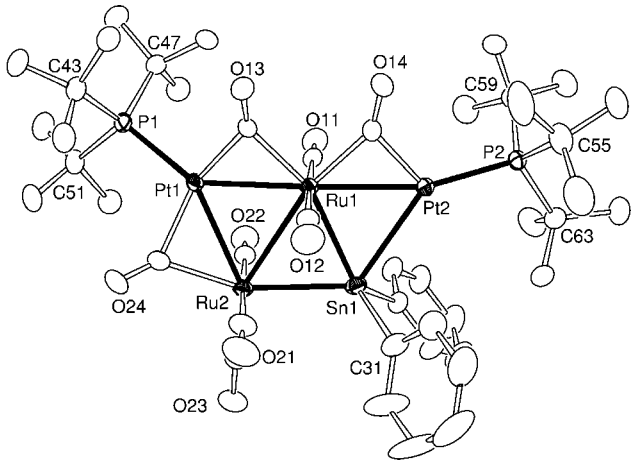

Figure 8. ORTEP diagram of the molecular structure of **5** showing 50% probability thermal ellipsoids. The hydrogen atoms are omitted for clarity. Selected interatomic bond distances (in Å) and angles (deg) are as follows: Ru(1)−Ru(2) = 2.9878(4), Ru(1)−Sn(1) = 2.6810(4), Ru(2)−Sn(1) = 2.6871(4), Ru(1)−Pt(1) = 2.7232(4), Ru(1)−Pt(2) = 2.7236(3), Ru(2)−Pt(1) = 2.7683(4), Pt(2)−Sn(1) = 2.8768(3), Pt(1)−P(1) = 2.3532(12), Pt(2)−P(2) = 2.3031(10); Ru(1)−Sn(1)−Pt(2) = 58.562(9), Ru(2)−Sn(1)−Pt(2) = 125.755(12), Ru(1)−Sn(1)−Ru(2) = 67.639(11), Pt(1)−Ru(1)−Pt(2) = 166.598(14).

distance in **5**, Ru(1)−Ru(2) = 2.9877(5) Å, is slightly shorter than that in **2**. These differences in the Ru−Ru bond distances are very small and are probably of no chemical significance. The added Pt(PBu^t_3) group bridges the Ru(1)−Sn(1) bond. Interestingly, the Ru(1)−Sn(1) bond is only very slightly shorter than the Ru(2)−Sn(1) bond: 2.6809(5) Å versus 2.6872(5) Å. Each Ru−Pt bond contains a bridging CO ligand. The two Ru−Pt bonds to Ru(1) are essentially equal in length: Ru(1)−Pt(1) = 2.7232(4) Å and Ru(1)−Pt(2) = 2.7236(3) Å. The Ru−Pt bond to Ru(2) is significantly longer than those to Ru(1): Ru(2)−Pt(1) = 2.7683(4) Å. The tin atom is pentavalent, and the Pt−Sn bond is long and presumably very weak. The Pt−Sn bond distance, 2.8768(3) Å, is significantly longer than the Ru(1)−Pt(2) bond distance and the Pt−Sn distances in the compounds Pt(H)($SnPh_3$)(PPh_3)$_2$ (Pt−Sn = 2.564(1) Å)[21] and $Os_3(CO)_9$[Pt(Ph)(PPh_3)$_2$](μ-$SnPh_2$)$_2$(μ_3-SnPh) (Pt−Sn = 2.6298(6) Å),[5] where the tin atom has the usual tetravalency. It is even longer than the Pt−Sn bond distances, 2.74−2.80 Å, found for Pt(PBu^t_3)-bridged Ru−Sn bonds in the series of compounds $Ru_3Sn_3Pt_n$ (n = 1−3), where the tin atom exhibits a similar pentavalency.[7]

To develop a view of the metal−metal bonding in **5**, its FH molecular orbitals were calculated.[15] The bulk of the metal−metal bonding in **5** is shown by the HOMO, HOMO-4, HOMO-13, and HOMO-18. These four orbitals are shown in Figure 9. The HOMO at −6.76 eV contains a large contour similar to that found in **4** that is delocalized across the platinum atom Pt(1) and the two ruthenium atoms. The HOMO-4 at −8.72 eV shows the bond between Pt(2) and Ru(1). The Ru−Sn bonding is revealed by HOMO-18 at −11.99 eV. The only orbital that exhibits any significant bonding interaction between Pt(2) and the tin atom is the HOMO-13 at −10.32 eV. The tin contribution to this orbital is relatively small and comes from the tin $5p_x$ orbital (8.2%) and $5p_y$ orbital (5.9%). This analysis is consistent

(21) Latif, L. A.; Eaborn, C.; Pidcock, A.; Ng, S. W. *J. Organomet. Chem.* **1994**, *474*, 217.

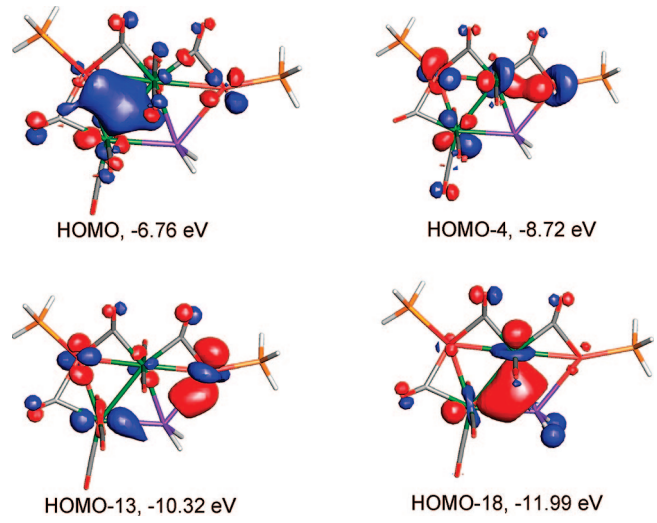

Figure 9. Contour diagrams of the FH molecular orbitals in **5** that show the metal−metal bonding.

Scheme 1

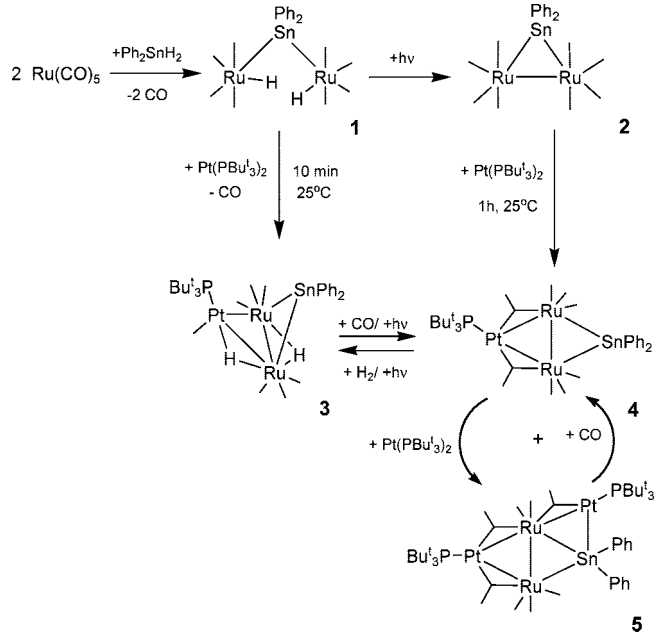

with a very weak Pt−Sn interaction, as indicated by the long Pt−Sn bond distance (see above).

Discussion

A summary of the reactions described in this report is shown in Scheme 1.

We have found that Ph_2SnH_2 reacts with 2 equiv of $Ru(CO)_5$ with the loss of CO and two oxidative addition steps to form the product **1**. In previous studies we found that $Ru(CO)_5$ reacts with Ph_3SnH by loss of a CO ligand and oxidative addition of the Sn−H bond to the ruthenium atom to form the compound $Ru(CO)_4(SnPh_3)H$ (**6**).[9] It seems likely that the formation of **1** is preceded by a product such as $Ru(CO)_4(SnPh_2H)H$, formed by the addition of 1 equiv of $Ru(CO)_5$ to Ph_2SnH_2, but this compound was not observed under our conditions. When irradiated, compound **1** eliminates H_2 to form compound **2**. The formation of H_2 was confirmed by ^1H NMR spectroscopy. The yield of **2** was increased when this reaction was performed under a CO atmosphere. To try to ascertain some information about

Scheme 2

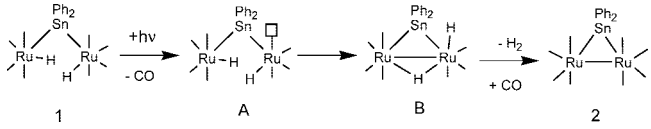

the mechanism of this reaction, we performed the irradiation of **1** under an atmosphere of ^{13}CO. We observed that ^{13}CO was incorporated significantly (on the average 20%) both in **2** and in the starting material **1**. We also found that ^{13}CO is readily incorporated into **2** when it is irradiated under an atmosphere of ^{13}CO, but we found no evidence for the formation of **1** from **2** in attempts to add H_2 to **2** under irradiation. This latter experiment indicates that the incorporation of ^{13}CO into **1** does not proceed through the intermediacy of **2**. On the basis of these results, the following mechanism for H_2 elimination from **1** to form **2** is proposed (see Scheme 2). In the first step a CO ligand is eliminated from one of the ruthenium atoms to give the intermediate **A**, which contains a vacant ligand site on one of the ruthenium atoms. This step is reversible and would thus explain the incorporation of ^{13}CO into **1** when the transformation is performed under a ^{13}CO atmosphere. In the second step, the $Ru(CO)_4H$ group in **A** is then oxidatively added to the unsaturated $Ru(CO)_3H$ group to form the intermediate **B**. A Ru−Ru bond would be formed at this time, and one or both of the hydride ligands could assume a position bridging the Ru−Ru bond. In the final step, CO is readded to the intermediate **B** and the product **2** is formed as the H_2 is eliminated. This step explains why the yield of **2** was higher when the reaction was preformed under a CO atmosphere. The addition of CO to **B** is very similar to the known reaction of $Os_3(CO)_{11}(\mu\text{-H})H$ with CO to yield $Os_3(CO)_{12}$ and H_2.[22] This mechanism is similar to the binuclear reductive elimination mechanism proposed by Norton for the elimination of H_2 from $Os(CO)_4H_2$ to yield the diosmium complex $Os_2(CO)_8H_2$.[23]

The products formed by the addition of the $Pt(PBu^t_3)$ group to the metal−metal bonds of **2** shows that the Ru−Ru bond is preferred over the Ru−Sn bonds but that both bonds are amenable to $Pt(PBu^t_3)$ addition. The preference for addition to the Ru−Ru bond is explained by the molecular orbital structure in **2**: that is, the most energetically accessible bond is the Ru−Ru bond, the HOMO. The Ru−Sn bonds are the next most available, HOMO-1 and HOMO-2 (see Figure 3).

Summary

In this work, the reactivity of Sn−H bonds with $Ru(CO)_5$ has been demonstrated through the reactions of the compound Ph_2SnH_2. It has been shown that both SnH bonds in Ph_2SnH_2 participate in the reaction to form the compound **1**, which then eliminates H_2 to form the $SnPh_2$-bridged diruthenium compound **2**. In addition, the ability of $Pt(PBu^t_3)_2$ to form heterometallic compounds containing tin has been further demonstrated. Compound **1** also reacts with $Pt(PBu^t_3)_2$ to form the trimetallic complex **3** by loss of CO. Compound **2** reacts with $Pt(PBu^t_3)_2$ to form the $Pt(PBu^t_3)$ adduct **4** by adding a $Pt(PBu^t_3)$ group to the Ru−Ru bond, and compound **4** reacts with $Pt(PBu^t_3)_2$ to form the $Pt(PBu^t_3)$ adduct **5** by adding a $Pt(PBu^t_3)$ group bridging one of its Ru−Sn bonds. Compound **4** reacts with hydrogen by loss of CO to form **3**.

As we have recently shown for related compounds, it is anticipated that these new heterometallic complexes will be able to serve as precursors to new nanoscale heterogeneous hydrogenation catalysts when deposited and activated on suitable supports.[2,7,24]

Acknowledgment. This research was supported by the National Science Foundation under Grant No. CHE-0743190. This report is dedicated to the memory of Professor F. Albert Cotton.

Supporting Information Available: CIF files for each of the structural analyses. This material is available free of charge via the Internet at http://pubs.acs.org.

OM800385W

(22) Deeming, A. J.; Hasso, S. *J. Organomet. Chem.* **1976**, *114*, 313–324.

(23) Norton, J. R. *Acc. Chem. Res.* **1979**, *12*, 139–145.

(24) (a) Thomas, J. M.; Adams, R. D.; Boswell, E. M.; Captain, B.; Grönbeck, H.; Raja, R. *Faraday Discuss.* **2008**, *138*, 301–315. (b) Adams, R. D.; Boswell, E. M.; Captain, B.; Hungria, A. B.; Midgley, P. A.; Raja, R.; Thomas, J. M. *Angew. Chem., Int. Ed.* **2007**, *46*, 8182–8185. (c) Hungria, A. B.; Raja, R.; Adams, R. D.; Captain, B.; Thomas, J. M.; Midgley, P. A.; Golvenko, V.; Johnson, B. F. G. *Angew. Chem., Int. Ed.* **2006**, *45*, 4782–4785.